Optical study of hydrogen-irradiated GaAsN/GaAs heterostructures

M. Geddo,[1,a)] M. Patrini,[1] G. Guizzetti,[1] M. Galli,[1] R. Trotta,[2] A. Polimeni,[2] M. Capizzi,[2] F. Martelli,[3] and S. Rubini[3]
[1]*Dipartimento di Fisica "A. Volta" and CNISM, Università degli Studi di Pavia, via Bassi 6, I-27100 Pavia, Italy*
[2]*Dipartimento di Fisica, Sapienza Università di Roma, P.le A. Moro 2, 00185 Roma, Italy*
[3]*Laboratorio Nazionale TASC-INFM-CNR, Area Science Park, S.S. 14, Km. 163.5, 34149 Trieste, Italy*

(Received 5 February 2011; accepted 5 May 2011; published online 20 June 2011)

The effect of hydrogen irradiation on the optical properties of $GaAs_{1-x}N_x$/GaAs heterostructures was investigated using photoreflectance and reflectance techniques. Systematic measurements performed on both as-grown and hydrogenated samples for N-concentrations ranging from 0.0% to 3.5% and for H-implanted doses from 3×10^{18} to 6×10^{18} ions/cm^2 have shown that (a) the H-induced widening of the energy gap is accompanied by a decrease of the refractive index of the H-treated samples with respect to the as-grown ones, resulting in an index mismatch that can be as large as 2% in the subgap spectral region; and (b) the presence of compressive strain in fully passivated GaAsN determines a decrease of the refractive index even below that of GaAs that can be eliminated via moderate thermal annealing. These findings are promising for the development of heterostructures with planar geometry, in which the simultaneous confinement of both carriers and photons, even on a nanometric scale, can be obtained in a single step process.
 [doi:10.1063/1.3597818]

I. INTRODUCTION

III-V nitrides, in particular GaAsN, have attracted great interest in recent years due to the possibility of modifying the electronic properties of the host lattice by incorporating a small percentage of nitrogen atoms.[1] Moreover, in III-V dilute nitrides, the electronic activity of nitrogen can be modulated through the formation of N–H complexes induced by hydrogen incorporation.[2–5] In GaAsN, the capability of tuning the band gap,[6] as well as the electron effective mass,[7] the exciton binding energy,[8] and the electron gyromagnetic factor,[9] via post-growth H-irradiation has been extensively studied. In addition, it was found that hydrogen produces a lattice expansion along the growth direction[5,10,11] that induces a reversal of the strain status of GaAsN layers. In this framework, photoreflectance (PR) and electroreflectance are powerful and practical techniques for studying the electronic and lattice properties of semiconductors within the same measurement. Indeed, they have been successfully employed in order to determine not only critical point energies in III-V dilute nitrides[1,8,10,12] but also strain-related valence band splitting in GaAsN/GaAs layers[13] and strain release in mismatched InGaAs/GaAs metamorphic buffers.[14]

Hydrogenation leads to potential applications in the field of planar optical devices via an in-plane modulation of the bandgap of GaAsN, as recently reported.[15–17] Moreover, it already has been shown[18] that the bandgap widening and the strain inversion due to deuterium implantation of $GaAs_{1-x}N_x$ with $x = 0.0122$ is accompanied by a variation Δn in the refractive index n of 0.8% to 0.4% in the 1.31 and 1.55 μm spectral regions of interest for fiber optic communications.

These promising results in view of the development of waveguides deserve further systematic investigation, especially regarding the extent of the Δn variation of the H-irradiated samples as a function of both N concentration and H dose, thus defining the real possibility of confining both carriers and photons, on a nanometric scale, with a single step process.

In this work, photoreflectance and reflectance (R) spectroscopies are used to investigate the effect of hydrogen incorporation on the optical properties of $GaAs_{1-x}N_x$ epitaxial layers for N concentrations in a wide range from 0.0% to 3.5% with a 3×10^{18} to 6×10^{18} ions/cm^2 H-implanted dose. All of the examined samples (as-grown and H-treated) are well characterized by taking advantage of the unique properties of the PR technique to simultaneously monitor the variation of the bandgap and the drastic change of the strain status of the GaAsN layer, as expected after hydrogenation. A detailed analysis of R spectra around the GaAsN bandgap permits one to follow its evolution with increasing N content and to determine the changes of the refractive index values upon H irradiation. The role of different N–H complexes in the optical response is also investigated.

II. EXPERIMENT

The heterostructures investigated have been grown on (001)-oriented GaAs substrates via plasma-assisted solid-source molecular beam epitaxy. They consist of a 500 nm thick GaAs buffer, a 100 nm thick $GaAs_{1-x}N_x$ layer (nominal concentrations: $x = 0.000$, 0.0068, 0.022, 0.031, 0.035), and a 20 nm thick GaAs cap layer.

N_2 cracking was obtained by using a radio frequency plasma source. A reference N-free GaAs epilayer grown under similar conditions was also measured. The layer

[a)]Author to whom correspondence should be addressed. Electronic mail: mario.geddo@unipv.it.

thickness was determined by means of reflection high-energy electron diffraction.

Post-growth treatment with atomic hydrogen was performed using ion-beam irradiation from a Kaufman source. Two different H doses were employed (3×10^{18} and 6×10^{18} ions/cm^2 for N concentrations smaller or greater than 3%, respectively) in order to ensure full N passivation in all samples.

PR measurements were performed at near-normal incidence in the 0.8–2.2 eV range, with a spectral resolution of 1 meV. The standard experimental apparatus[19] was operated with a 100 W halogen lamp as a probe source. The excitation source was provided by a 20 mW Coherent sapphire-488 nm laser, mechanically chopped at a frequency of 220 Hz.

R measurements in the 0.2-1.65 μm wavelength range were performed at near-normal incidence with a double-beam spectrophotometer (Cary Varian 6000i) with a photometric accuracy of 0.5% and a spectral resolution better than 1 nm. An Al mirror covered with MgF_2 film, the absolute reflectivity of which was directly measured, was used as reference.

Atomic force microscope (AFM) images were obtained with a Thermo Microscope CPII AFM operated in tapping mode with NT-MDT silicon tips. Data analysis (width and height calculations on the line profiles) was carried out with Image Processing and Data Analysis software, version 2.1.15, from TM Microscopes

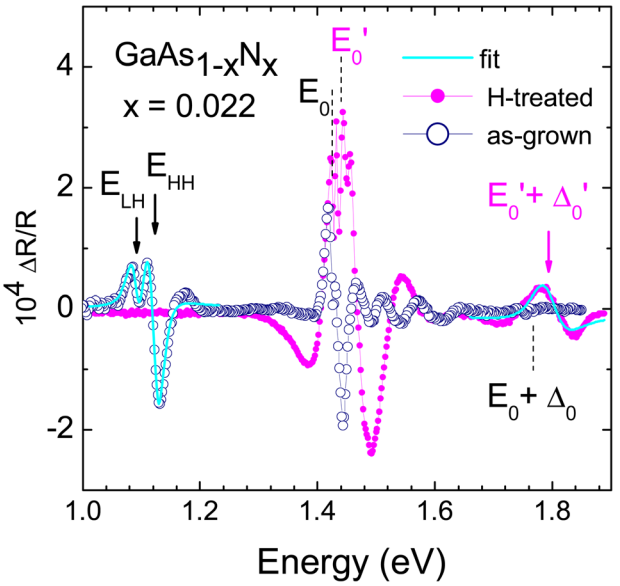

FIG. 1. (Color online) Room-temperature PR spectra of the as-grown (open circles) and H-treated (solid circles) samples with $x = 0.022$. Features near 1.1 eV are related to the red-shifted GaAsN fundamental gap ($E-$) and highlight the doublet (E_{LH} and E_{HH}) arising from the tensile strain in the as-grown GaAsN epitaxial layers. These features vanish in the spectrum of the H-treated sample. Moreover, the transition energies E'_0 and $E'_0 + \Delta'_0$ (associated with the bandgap and the SO band of the GaAsN:H layers) are blue-shifted with respect to the corresponding GaAs transitions, giving evidence that strain inversion has occurred. The arrows mark the transition energies, as obtained from the best fit (solid line) to the experimental line shape.

III. RESULTS AND DISCUSSION

A. PR results: GaAsN electronic and strain properties

Both the electronic and the structural properties of the $GaAs_{1-x}N_x$ layers were checked using PR. In particular, the analysis of the experimental PR line shape allows for the measuring of the energy of the fundamental band gap[12] and the tensile strain[10,11] in the as-grown $GaAs_{1-x}N_x$ layers, as well as the bandgap recovery[8,10] and the strain inversion[5,11,18] in the H-treated samples. A typical example is shown in Fig. 1, in which the room-temperature PR spectra in the 1.0–1.9 eV energy range are displayed for the as-grown (open circles) and H-treated (solid circles) samples with $x = 0.022$.

The two features near 1.10 eV (E_{LH} and E_{HH}) in the low-energy part of the spectrum of the as-grown sample are related to the GaAsN fundamental energy gap.[12] Epitaxial $GaAs_{1-x}N_x$ layers grown on (100) GaAs substrate are under biaxial tensile strain.[10,11] The doublet is the signature of the strained status of the GaAsN layers. We assign the first and the second feature to the split light- and heavy-hole $E-$ transitions in the GaAsN layer,[18] respectively. The spectral features near 1.42 eV are related to the bandgap E_0 of the GaAs cap/buffer layers and exhibit the typical Franz-Keldysh oscillations.[20] The high-energy part of the spectrum displays a less intense structure near 1.76 eV that we assign to the split-off transition $E_0 + \Delta_0$ in the GaAs cap/buffer layers.[20,21]

In the case of the H-irradiated $GaAs_{1-x}N_x$ sample, all of the spectral features related to the N electronic activity vanish, and the spectrum assumes a GaAs-like behavior. The corresponding features are stronger than those coming from the GaAs cap/buffer layers, and are much broader, as is usually found in the PR spectra of H- or D-treated dilute nitrides.[8,10,18] Moreover, the energies of the GaAsN:H fundamental gap E'_0 (~1.44 eV) and of the split-off transition $E'_0 + \Delta'_0$ (~1.79 eV) are blue-shifted with respect to those expected from the full passivation of N atoms alone. These occurrences indicate the presence of a H-induced compressive strain in the hydrogenated sample[5,10,11,18] due to the lattice expansion caused by the formation of N–H complexes.[3,11]

The transition energies E_{HH}, E_{LH}, and $E'_0 + \Delta'_0$ have been obtained from the best fit (solid line) to the experimental line shape (symbols) by using, for each PR feature, the appropriate Aspnes functional form.[18,21] This analysis provides us with fine information about the composition and the strain status of the GaAsN layers. As a matter of fact, according to the deformation potentials theory,[22] the energy gaps associated with the transitions from heavy-hole (HH), light-hole (LH), and split-off (SO) bands to the conduction band, as well as the valence band splitting $\Delta E = E_{HH} - E_{LH}$, can be related[14] to the in-plane strain $\varepsilon_{//} = (a_0 - a_x)/a_x$, where a_0 and a_x are the GaAs and the *free-standing* (or *relaxed*) $GaAs_{1-x}N_x$ lattice parameters, respectively. As an example, in the case of the untreated $x = 0.022$ sample (see Fig. 1, solid lines), we obtain $E_{HH} = 1.123$ eV and $E_{LH} = 1.092$ eV, with $\Delta E = 31$ meV. By using the procedure explained in more detail in Ref. 18, we get $\varepsilon_{//} = 0.0039$, which has to be compared with $\varepsilon_{//} = 0.0045$, the expected tensile in-plane strain for coherent growth. At the same time, by using the

experimental value of the split-off transition energy $E'_0+\Delta'_0=1.792\pm0.002$ eV, as obtained from the best fit, we get an estimate of the compressive strain $\varepsilon_{//}=-0.0027$ in the GaAsN:H layer from the extent of the blue-shift[18] (25 meV) of the SO band with respect to the corresponding band in pure GaAs.[23] The sign reversal of $\varepsilon_{//}$ observed after H incorporation nicely agrees with previous x-ray diffraction studies.[5,11]

In Fig. 2, the N-dependence of the transition energies E_{HH} and E_{LH} (thin lines) for pseudomorphic GaAsN, calculated by applying the deformation potential theory to the $E-$ band predicted by the band anticrossing (BAC) model[12] (thick solid line), is compared to the PR derived results (squares). In these calculations, the elastic stiffness constants (C_{11} and C_{12}) and the band parameter values of the $GaAs_{1-x}N_x$ alloy were obtained via linear interpolation between the end-binary material values of GaAs and GaN.[24] As shown, with increasing N concentration, the measured ΔE is systematically smaller than the corresponding one calculated for coherent growth, consistent with the reduction of the critical thickness for plastic relaxation due to the enhanced material mismatch. Moreover, for intermediate N concentrations, the nominal values are clearly overestimated. Anyway, taking into account the partially relaxed nature of the GaAsN layers, the agreement between energy gap PR values at nominal composition and the N-dependence of the bandgap derived from the literature data[1,24] on dilute nitrides is within 10%. We note that this uncertainty regarding N concentration is a fact of minor importance in the context of our investigations.

The GaAsN bandgap energies E_0 (solid circles) after H-irradiation, as estimated from a simulation of the PR spectra, are also displayed in Fig. 2 and are compared to the GaAs fundamental gap E_0. The calculated blue-shift of the fundamental gap (more precisely, of its HH related spectral feature) and of the split-off transition energies versus the in-plane compressive strain are shown for GaAs in the inset of Fig. 2. As reported elsewhere,[18] assuming for the passivated GaAsN the same stiffness constants and band parameters as in GaAs, the compressive strain of the layer can be estimated by using the strain dependence of the blue-shift of the fundamental gap or (preferably) of the split-off band.

The PR results can be summarized as follows:

(a) All of the as-grown samples present PR evidence of in-plane tensile strain in $GaAs_{1-x}N_x$ layers, except for $x=0.035$, where the line shape's broadening prevents any valence band splitting evaluation. In particular, from the experimental value of ΔE we infer that for $x=0.0068$, the layer is fully strained; for $x=0.022$, the layer is 14% relaxed; for $x=0.031$, the layer is 44% relaxed; and for $x=0.035$ (ΔE not detectable), the layer is almost completely relaxed.

(b) All of the H-treated samples show evidence of full recovery of the bandgap of the host lattice (i.e., GaAs), as well as of the in-plane compressive strain, in $GaAs_{1-x}N_x$ layers ranging from $\varepsilon_{//}=-0.0008$ for $x=0.0068$ to $\varepsilon_{//}=-0.0035$ for $x=0.035$. This provides evidence that strain inversion occurred after H-irradiation.

B. Reflectance measurements and AFM images

In Fig. 3, the interband R spectra of the as-grown samples are shown. The optical response of the N-free ($x=0.000$) sample is also shown. The effect of the composition in the GaAsN layers on the dispersive R line shape at the fundamental gap (E_0 near 0.88 μm ~ 1.40 eV for $x=0$) is highlighted by the red-shift of the corresponding spectral features ($E-$) for increasing N concentrations, consistent with PR results. In contrast, the energy position of higher interband transitions (E_1 and $E_1+\Delta_1$) is scarcely affected by N, in agreement with results from the literature.[1] The weak blue-shift undergone by higher interband transitions, due to

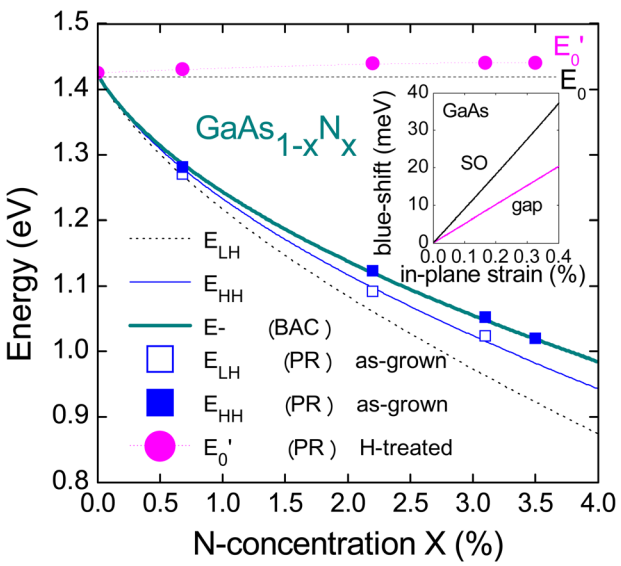

FIG. 2. (Color online) N-dependence of the GaAsN transition energies E_{HH} and E_{LH} (thin solid lines) calculated by applying the deformation potentials theory to the $E-$ band predicted by the BAC model (thick solid line). Squares mark the PR results for the as-grown samples. The GaAsN:H bandgap energies E'_0 (solid circles), as estimated from a simulation of the PR spectra, are also reported and compared to the GaAs value (E_0). In the inset, the expected blue-shift of the GaAs bandgap and split-off band are plotted vs the in-plane compressive strain.

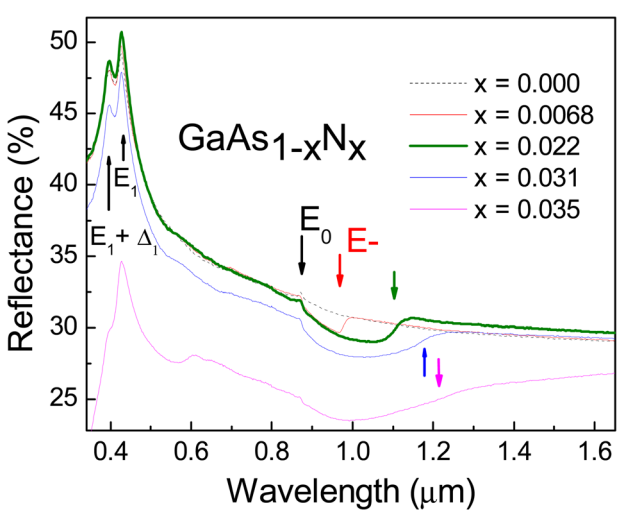

FIG. 3. (Color online) Room-temperature reflectance spectra of as-grown $GaAs_{1-x}N_x$ samples with different N contents. The arrows mark the main interband transition energies of the GaAsN and GaAs layers.

the combination of strain and compositional effects, becomes evident only for higher N concentrations.[1,25] We note that the intensity of the spectral features decreases drastically for samples with higher N concentrations ($x = 0.031$ and $x = 0.035$). This can be attributed to the presence of surface roughness, which has been evidenced by AFM measurements of the same samples.

In Fig. 4, AFM images of the as-grown samples for $x = 0.000$ and $x = 0.035$ are shown. The significant deepness and extension of the surface irregularities of the $x = 0.035$ sample might account for the drastic decrease of the intensity of the R spectral features. Nevertheless, it must be said that the R reduction does not follow the typical ($\propto 1/\lambda^4$) scattering behavior, and instead includes a quasi-rigid shift (see Fig. 3). We can explain this behavior by noticing that for samples with greater concentrations ($x = 0.035$ and $x = 0.031$), the photoluminescence (PL) and PR results seem to indicate the likely presence of phase-separated regions of micrometric dimensions that, in turn, might produce surface irregularities and hence a decrease of the R signal.

In more depth, we may consider as an example the optical data shown in Fig. 5, in which the room temperature PR spectra in the 0.8-1.7 eV range are displayed for the as-grown (open circles) and H-treated (solid circles) samples with $x = 0.031$. Features near 1.05 eV are related to the red-shifted GaAsN fundamental gap ($E-$) and highlight the doublet (E_{LH} and E_{HH}) arising from the tensile strain in the as-grown GaAsN epitaxial layers. Due to H irradiation, these features vanish in the spectrum of the H-treated sample, and the fundamental gap PR features assume a GaAs-like energy position, as with the sample with $x = 0.022$ (shown in Fig. 1) and all of the other examined samples. In contrast, a new feature ($E-'$) grows up near 1.2 eV. This feature, due to its energy position, must be related to the signal coming from regions of the GaAsN layer with an effective N concentration of about 1%, indicating the presence of not fully passivated N. Similar behavior was also observed for the sample with $x = 0.035$. This could be due either to a non-homogeneous in-depth distribution of H (Ref. 26) (discussed in more detail in the next subsection) or to in-plane N-richer regions, as suggested above. In any case, for $x > 3\%$, the R signal cannot be properly used or modeled in order to extract the optical parameters of interest.

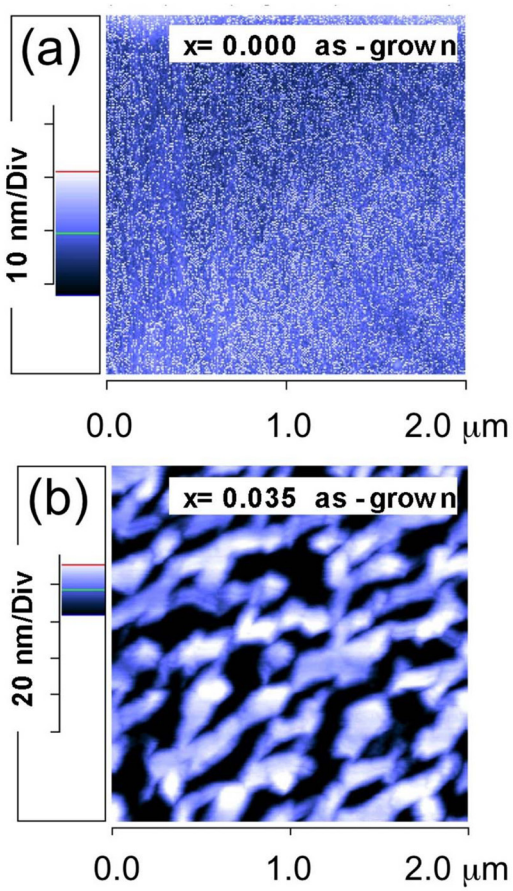

FIG. 4. (Color online) AFM images of as-grown $GaAs_{1-x}N_x$ samples for (a) $x = 0.000$ (b) and $x = 0.035$, showing the surface texturing of the two samples.

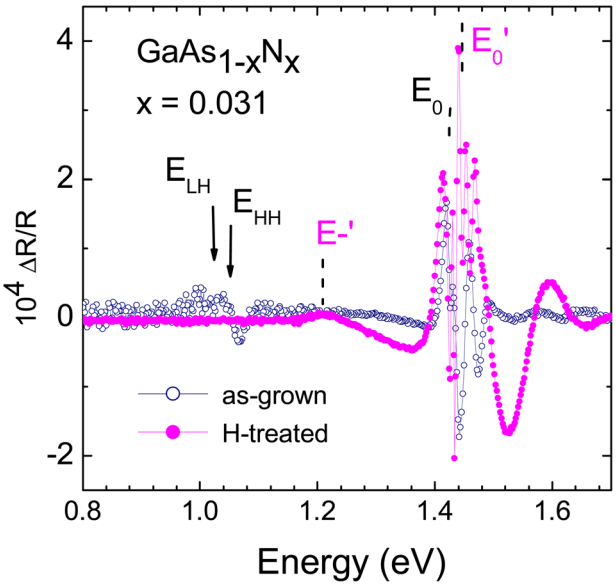

FIG. 5. (Color online) Room-temperature PR spectra of the as-grown (open circles) and H-treated (solid circles) samples with $x = 0.031$. Features near 1.05 eV are related to the red-shifted GaAsN fundamental gap ($E-$) and highlight the doublet (E_{LH} and E_{HH}) arising from the tensile strain in the as-grown GaAsN epitaxial layers. Due to H irradiation, these features vanish in the spectrum of the H-treated sample, as observed for the sample with $x = 0.022$ (see Fig. 1). In contrast, a new feature ($E-'$) appears near 1.2 eV. This feature, originating from not fully passivated N, indicates the presence of phase-separated regions of micrometric dimensions (see text). The arrows mark the transition energies, as obtained from the best fit to the experimental line shape.

The comparison of the R spectra before and after H-treatment is shown in Fig. 6. It is evident that H-treated samples recover the R response typical of the GaAs-like fundamental gap, centered at 0.88 μm (~1.4 eV), in agreement with PR results. Moreover, at the same time, H irradiation decreases the reflectance of the multilayer sample structure in the subgap spectral region. This effect is more pronounced for increasing N concentrations. Because GaAs optical properties are not affected by H irradiation,[11] this effect ought to be attributed to the increase of the refractive index in H-treated GaAsN layers.

At this point, one may ask for the effect of H irradiation on the surface roughness of the examined samples.

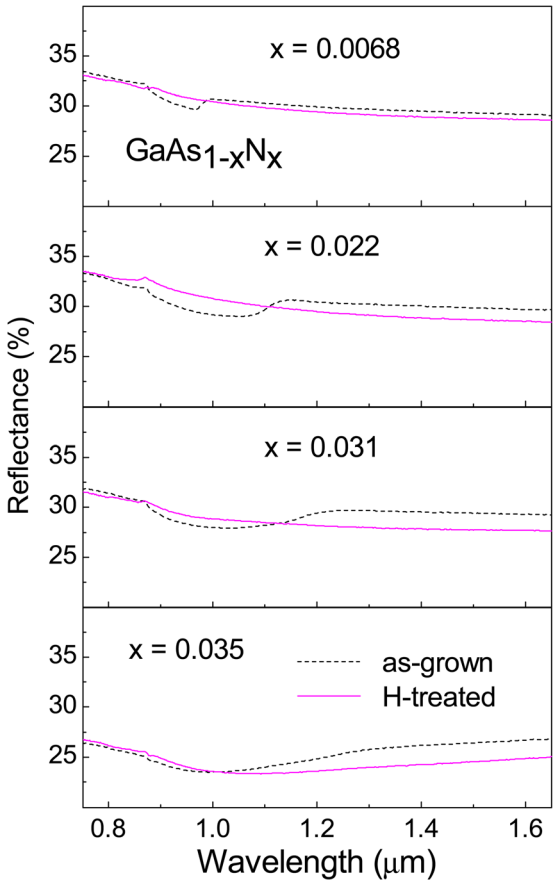

FIG. 6. (Color online) Comparison of the room-temperature reflectance spectra of $GaAs_{1-x}N_x$ samples before and after H-treatment. Note the systematic decreasing of the reflectance values, in the sub-gap spectral region, after hydrogenation. This effect is exalted for increasing N content.

Systematic AFM measurements have proved that no significant variation of the surface irregularities occurs after H-treatment, suggesting that the surface roughness increases with N content, nearly independent from H irradiation, although it becomes significant, to the point of drastically modifying R behavior, only for N concentrations much greater than 2%.

C. Reflectance spectra analysis and refractive index determination in GaAsN and GaAsN:H

Reflectance spectra allow the determination of the refractive index changes due to N alloying and subsequent hydrogenation procedures.[18] In order to obtain the refractive index $n(\lambda)$ of the as-grown and hydrogenated GaAsN layers in the subgap region, a best-fit procedure using the R spectra was performed with the software package WVASE32® (J.A. Woollam Co. Inc.), based on the Levenberg–Marquardt algorithm. The multilayer structure of the samples was modeled with a five-phase scheme: air/2 nm oxide overlayer/20 nm GaAs cap/100 nm GaAsN/infinite GaAs buffer and substrate. With regard to the oxide overlayer, we assumed the dielectric function of the Ga_2O_3 native oxide[27] and estimated its effective thickness by best-fitting the higher energy region (4–5 eV) of spectroscopic ellipsometry curves taken on the samples. The dielectric function used for the GaAs cap, buffer, and substrate layers was taken from the literature.[28] We verified that this precisely reproduces our measurements of the reference N-free GaAs epilayer.[18] The dielectric function of the GaAs cap/buffer layers was assumed not to change upon hydrogenation. This assumption relies on secondary-ion mass spectrometry,[29] which demonstrates that H incorporation is an efficient process in the N-doped layer, whereas it is negligible outside the dilute nitride film.

The $n(\lambda)$ dispersion of $GaAs_{1-x}N_x$ and hydrogenated $GaAs_{1-x}N_x$ layers in the subgap transparency region was modeled through the Sellmeier relation[30] $n^2 = A + B\lambda^2/(\lambda^2 - C) + D\lambda^2/(\lambda^2 - E)$, where A was fixed; B, C, D, and E were the free-variable parameters of the best-fit to the R spectra; and λ was the wavelength (in μm).

We have noticed before that AFM measurements have shown a relevant surface roughness in the samples with higher N concentrations. However, PR and PL results indicate an inhomogeneous N distribution that might account for the unusual behavior of the R spectra. Furthermore, in samples with a high N concentration and a relatively large thickness (> 200 nm), the strongly trapping-limited diffusion of H (and the corresponding very sharp profile)[26,29] leads to the formation of two regions along the axis of crystal growth: one region (closer to the surface) having the bandgap of GaAs (namely, fully passivated GaAsN), and a second (usually a much thinner region farther from the surface) with the bandgap of as-grown GaAsN.[29] This accounts for a PR feature near 1.2 eV, clearly revealed by the PR spectrum of the H-treated sample with $x = 0.035$ and assigned to N atoms that remain electrically active (not shown here). The same occurrence, although less evident, seems to characterize the sample with $x = 0.031$, too. The presence of non-passivated N in the H-treated sample with $x = 0.035$ has been confirmed by Raman shift measurements (not shown here). All of these facts make the use of Sellmeier modeling inappropriate;[30] consequently, we applied this procedure only to samples with low N concentrations ($x = 0.000$, 0.0068, and 0.022), both as-grown and H-treated.

The $GaAs_{1-x}N_x$ refractive index behavior, as obtained from the best fit to the R spectra in the 1.2–1.65 μm wavelength range, for $x = 0.000$, $x = 0.0068$, and $x = 0.022$ is shown in Fig. 7. The overall refractive index increment with

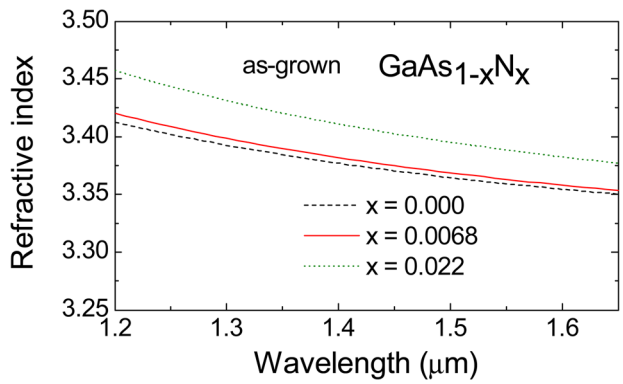

FIG. 7. (Color online) Refractive index spectra for $GaAs_{1-x}N_x$ as-grown samples with different N contents, as obtained from the best fit to the R spectra in the subgap region.

increasing N concentration is evident. Our results are in moderate agreement with previous ellipsometric measurements[31] performed on MOVPE grown tensile strained GaAsN layers of similar compositions.

In Figs. 8(a) and 8(b), the effect of H irradiation on the GaAsN refractive index is shown for the $x = 0.0068$ and $x = 0.022$ samples, respectively, and is compared to the N-free GaAs refractive index data. For $x = 0.0068$, H irradiation results in an overall relative reduction of the refractive index by (1-0.6)% in the wavelength range from $\lambda = 1.3$ to 1.55 μm. For $x = 0.022$, the overall relative reduction of the refractive index is increased to (2–1.5)% in the same wavelength range. These values of the refractive-index change nicely fulfill those required for waveguiding in planar integrated optical devices.[32] This effect can be engineered for in-plane confinement using N concentration and post-growth H-irradiation as external tunable parameters. As an example, recently it has been shown that the deposition of patterned metallic masks onto the surface of GaAsN/GaAs heterostructures enables the production of micrometric stripe-like adjacent regions in the GaAsN growth plane with a sizable mismatch in the bandgap,[16] refractive index,[18] and strain status.[33] We note here that a larger refractive index change Δn could be obtained by using GaAsN layers with a higher N concentration. However, this is true as long as the optical quality of the materials is not degraded by the presence of fluctuations highlighted by PR, PL, and AFM measurements. The overall approach has been improved on the nanometric scale by obtaining well-defined GaAsN wires in GaAsN:H layers with a sharp diffusion profile for H (or deuterium).[15–17,26]

Very interesting, we note in Fig. 8 that upon H-irradiation, the values of the refractive index of the GaAsN layers for wavelengths $\lambda > 1$ μm are significantly *lower* than those of the host matrix (n overshooting). This behavior is well described in Fig. 9, in which the absolute variation of the GaAsN refractive index after H irradiation $\Delta n = n_{GaAsN} - n_{GaAsN:H}$, as obtained from the best fit of the reflectance data, is displayed for $\lambda = 1.31$ μm (squares). The difference between the refractive index of GaAsN and that of N-free GaAs, i.e., $\Delta n' = n_{GaAsN} - n_{GaAs}$ as obtained in this work and as derived from the optical data reported in Ref. 31 (solid and open circles, respectively), is also shown for the same wavelength.

The reason for the refractive index reduction (and its intriguing overshooting) in H-treated GaAsN, as occurred for many other electronic and structural properties of dilute nitrides,[1,2,7,9,8,6,10,11] may be related to the formation of different types of hydrogen complexes. It is now well established that the bandgap recovery and the lattice overshooting in H-treated GaAsN layers are related to N-2 H and N-3 H complexes, respectively.[5] Each one of these complexes is characterized by a different concentration ratio [H]/[N] and a different activation energy.[5,34]

To gain deeper insight into the role played by the different complexes, we repeated the R measurements on the H-treated samples after moderate annealing.[5,34] This process has proved to give [H]/[N] = 2, removing the more weakly bound hydrogen atoms and consequently turning N-3 H complexes into N-2 H complexes, with the former being responsible for the compressive strain observed in H irradiated GaAsN layers.[5,11,18] In contrast, it has been shown that the electronic passivation of N atoms due to N-2 H complexes is still active after the thermal treatment.

After a 5 h annealing at 225 °C, we observed an increase of the reflectance of the hydrogenated GaAsN/GaAs structures, and R values in the subgap region become closer to those characterizing the sample with $x = 0.000$. An example is shown in Fig. 10, in which the R spectra for the sample with $x = 0.022$ (as-grown, H irradiated, before and after annealing) are compared with the spectrum of the sample

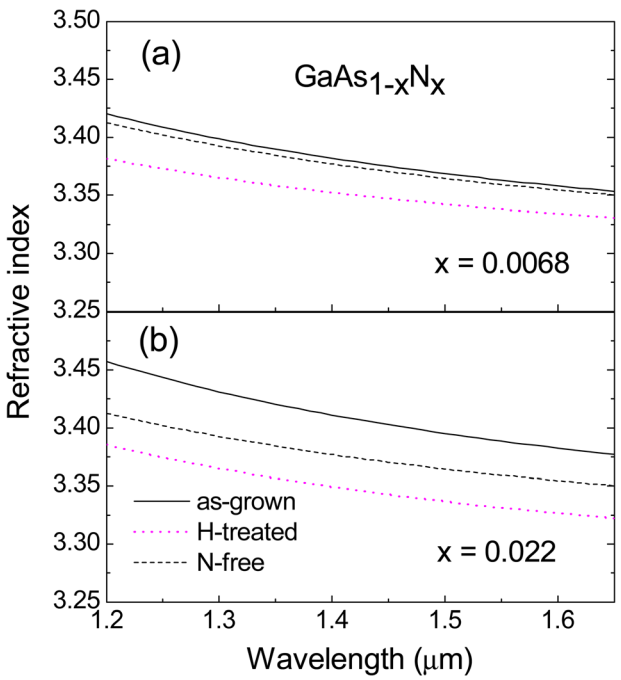

FIG. 8. (Color online) $GaAs_{1-x}N_x$ refractive index spectra before and after H irradiation, as obtained from the best fit to the R spectra in the subgap region for (a) $x = 0.0068$ and (b) $x = 0.022$ samples. The dashed lines report the GaAs as-grown sample values.

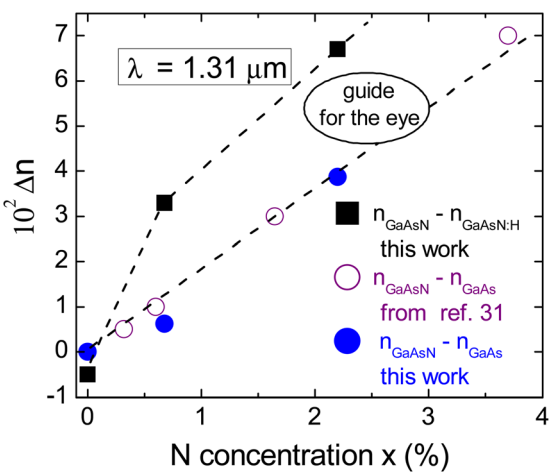

FIG. 9. (Color online) Refractive index variation Δn in $GaAs_{1-x}N_x$ layers at $\lambda = 1.31$ μm after H irradiation (squares). The difference $\Delta n'$, at the same wavelength, between the refractive index of the $GaAs_{1-x}N_x$ layers and that of GaAs derived in this work and from the optical data reported in Ref. 31 are also shown (circles).

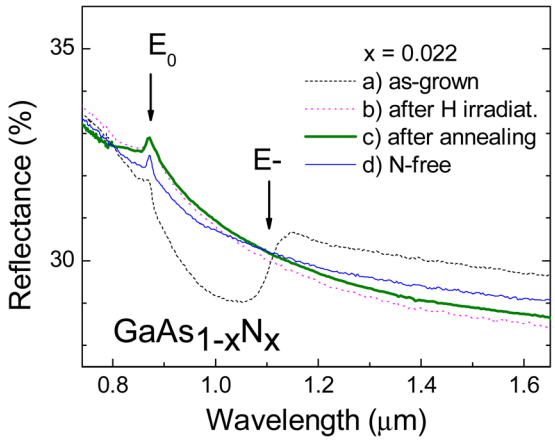

FIG. 10. (Color online) Reflectance spectra for the $GaAs_{1-x}N_x$ sample with $x = 0.022$: (a) as-grown, (b) H irradiated before annealing, and (c) H irradiated after annealing. Note the slight increase of R in the sub-gap spectral region after annealing, approaching the values of GaAs (N-free sample) reported for comparison in line (d).

with $x = 0.000$, i.e., GaAs material without compressive strain. Moreover, the PR measurements exhibit a red-shift of few meV of the PR features associated with the bandgap (E'_0) and the split-off band ($E'_0 + \Delta'_0$), highlighting the fact that a moderate reduction of the compressive strain in the hydrogenated GaAsN layers[18] occurred after annealing. In contrast, no variation was detected after annealing for the R and PR spectra of the sample with $x = 0.000$.

Because the thermal treatment does not affect the refractive index (or the strain status) of GaAs, we can infer that the increase of the refractive index of the hydrogenated GaAsN layer following annealing produces the increase of the reflectance of the whole GaAsN/GaAs heterostructure. Consequently, the refractive index behavior can be explained as follows: H irradiation reduces the refractive index of GaAsN to values *lower* than those characterizing GaAs in the subgap region (*n* overshooting). This is due to the formation of N-3 H complexes. After thermal treatment at 225 °C, the more weakly bound hydrogen is partially removed,[5,34] inducing the observed reduction of the compressive strain and, at the same time, the observed increase of the sample's R (and of the refractive index of the GaAsN layers). Due to the observed tendency of the *n* overshooting to vanish with the reduction of the concentration of N-3 H complexes, we conclude that the latter are responsible for this phenomenon. Then, a suitable post-growth thermal treatment might drive the refractive index of the hydrogenated GaAsN layers to make it coincide with that of GaAs.

IV. CONCLUSIONS

We have investigated the relevant changes induced by hydrogen irradiation in the optical properties of GaAsN by means of reflectance-based spectroscopy. The bandgap recovery, as well as the presence of a peculiar compressive strain resulting from H irradiation in dilute GaAsN, highlighted by PR spectra, has been shown to be accompanied by a reduction of 1% or more of the refractive index in the 1.31 and 1.55 μm spectral windows of interest for fiber optic communications. Moreover, the role played by different hydrogen complexes in determining the refractive index behavior in GaAsN dilute nitride has been clarified.

These results provide us with an opportunity to modulate the refractive index of GaAsN by means of post-growth treatments and, taking advantage of the extent of the refractive index change, indicate a single step process for the simultaneous confinement of photons and charge carriers in GaAsN/GaAs heterostructures. The observed changes in the refractive index are such to envision the future development of waveguides and/or optical couplers integrated with light emitting devices, and they could have relevance with regard to the realization of integrated optical circuits.

ACKNOWLEDGMENTS

This work was partly supported by the Italian Ministry of University and Research, FIRB Contract No. RBAP06L4S5.

[1]For a review see *Physics and Applications of Dilute Nitrides*, edited by I. A. Buyanova and W. M. Chen (Taylor & Francis, New York, 2004), and *Dilute Nitride Semiconductors*, edited by M. Henini (Elsevier, Oxford, England, 2005).
[2]A. Polimeni, G. Baldassarri H. v., H. M. Bissiri, M. Capizzi, M. Fischer, M. Reinhardt, and A. Forchel, Phys. Rev. B **63**, 201304(R) (2001).
[3]F. Jiang, M. Stavola, M. Capizzi, A. Polimeni, A. Amore Bonapasta, and F. Filippone, Phys. Rev. B **69**, 041309(R) (2004).
[4]G. Ciatto, F. Boscherini, A. Amore Bonapasta, F. Filippone, A. Polimeni, and M. Capizzi, Phys. Rev. B **71**, 201301 (2005).
[5]M. Berti, G. Bisognin, D. De Salvador, E. Napolitani, S. Vangelista, A. Polimeni, M. Capizzi, F. Boscherini, G. Ciatto, S. Rubini, F. Martelli, and A. Franciosi, Phys. Rev. B **76**, 205323 (2007).
[6]M. Felici, A. Polimeni, G. Salviati, L. Lazzarini, N. Armani, F. Masia, M. Capizzi, F. Martelli, M. Lazzarino, G. Bais, M. Piccin, S. Rubini, and A. Franciosi, Adv. Mater. **18**, 1993 (2006).
[7]F. Masia, G. Pettinari, A. Polimeni, M. Felici, A. Miriametro, M. Capizzi, A. Lindsay, S. B. Healy, E. P. O'Reilly, A. Cristofoli, G. Bais, M. Piccin, S. Rubini, F. Martelli, A. Franciosi, P. J. Klar, K. Volz, and W. Stoltz, Phys. Rev. B **73**, 73201 (2006).
[8]M. Geddo, R. Pezzuto, M. Capizzi, A. Polimeni, M. Fischer, and A. Forchel, Eur. Phys. J. B **30**, 39 (2002).
[9]G. Pettinari, F. Masia, A. Polimeni, M. Felici, A. Frova, M. Capizzi, A. Lindsay, S. B. Healy, E. P. O'Reilly, P. J. Klar, W. Stolz, A. Cristofoli, G. Bais, M. Piccin, S. Rubini, F. Martelli, and A. Franciosi, Phys. Rev. B **74**, 245202 (2006).
[10]P. J. Klar, H. Gruning, M. Gungerich, W. Heimbrodt, J. Koch, T. Torunski, W. Stolz, A. Polimeni, and M. Capizzi, Phys. Rev. B **67**, 121206(R) (2003).
[11]G. Bisognin, D. De Salvador, A. V. Drigo, E. Napolitani, A. Sambo, M. Berti, A. Polimeni, M. Felici, M. Felici, M. Capizzi, M. Grungerich, P. J. Klar, G. Bais, F. Jabeen, M. Piccin, S. Rubini, F. Martelli, and A. Franciosi, Appl. Phys. Lett. **89**, 061904 (2006).
[12]W. Shan, W. Walukiewicz, J. W. Ager III, E. E. Haller, J. F. Geisz, D. J. Friedman, J. M. Olson, and S. R. Kurtz, Phys. Rev. Lett. **82**, 1221 (1999); Phys. Rev. B **62**, 4211 (2000).
[13]Y. Zhang, A. Mascarenhas, H. P. Xin, and C. W. Tu, Phys. Rev. B **61**, 4433 (2000);M. H. Ya, Y. F. Chen, and Y. S. Huang, J. Appl. Phys. **92**, 1446 (2002);J. Ibanez, R. Kudrawiec, J. Misiewicz, M. Schimdbauer, M. Henini, and M. Hopkinson, *ibid.* **100**, 093522 (2006).
[14]M. Geddo, G. Guizzetti, M. Patrini, T. Ciabattoni, L. Serravalli, P. Frigeri, and S. Franchi, Appl. Phys. Lett. **87**, 263120 (2005).
[15]L. Felisari, V. Grillo, F. Martelli, R. Trotta, A. Polimeni, M. Capizzi, F. Jabeen, and L. Mariucci, Appl. Phys. Lett. **93**, 102116 (2008).
[16]R. Trotta, A. Polimeni, M. Capizzi, D. Giubertoni, M. Bersani, G. Bisognin, M. Berti, S. Rubini, F. Martelli, L. Mariucci, M. Francardi, and A. Gerardino, Appl. Phys. Lett. **92**, 221901 (2008).
[17]R. Trotta, L. Cavigli, L. Felisari, A. Polimeni, A. Vinattieri, M. Gurioli, M. Capizzi, F. Martelli, S. Rubini, L. Mariucci, M. Francardi, and A. Gerardino, Phys. Rev. B **81**, 235327 (2010).

[18]M. Geddo, T. Ciabattoni, G. Guizzetti, M. Galli, M. Patrini, A. Polimeni, R. Trotta, M. Capizzi, G. Bais, M. Piccini, S. Rubini, F. Martelli, and A. Franciosi, Appl. Phys. Lett. **90**, 091907 (2007).
[19]M. Geddo, G. Guizzetti, M. Capizzi, A. Polimeni, D. Gollub, and A. Forchel, Appl. Phys. Lett. **83**, 470 (2003).
[20]D. E. Aspnes and A. A. Studna, Phys. Rev. B **7**, 4605 (1973); D. E. Aspnes, Phys. Rev. B **10**, 4228 (1974).
[21]D. E. Aspnes, Surf. Sci. **37**, 418 (1973).
[22]F. H. Pollak, in *Semiconductors and Semimetals*, edited by T. P. Pearsall (Academic, Boston, 1990), Vol. 32, p. 17; F. H. Pollak and M. Cardona, Phys. Rev. **172**, 816 (1968).
[23]The SO energy was also checked for a GaAs buffer layer grown on a 001 GaAs substrate under similar conditions. We obtained $E_0+\Delta_0 = (1.767 \pm 0.001)$ eV. We note that the broadening of the E_0' feature and the signals' overlapping reduce the accuracy of the estimate of the E_0' transition energy and hamper the estimation of any valence band splitting.
[24]I. Vurgaftman and J. R. Meyer, J. Appl. Phys. **94**, 3675 (2003).
[25]G. Leibiger, V. Gottshalch, B. Rheinlander, J. Sik, and M. Schubert, Appl. Phys. Lett. **77**, 1650 (2000).
[26]R. Trotta, D. Giubertoni, A. Polimeni, M. Bersani, M. Capizzi, F. Martelli, S. Rubini, G. Bisognin, and M. Berti, Phys. Rev. B **80**, 195206 (2009).
[27]G. Ghosh, *Handbook of Thermo-Optic Coefficients of Optical Materials with Applications* (Academic, San Diego, 1998), Chap. 2.
[28]S. Zollner, Appl. Phys. Lett. **63**, 2523 (1993).
[29]R. Trotta, A. Polimeni, M. Capizzi, D. Giubertoni, M. Bersani, G. Bisognin, M. Berti, S. Rubini, F. Martelli, L. Mariucci, M. Francardi, and A. Gerardino, Appl. Phys. Lett. **92**, 221901 (2008).
[30]S. Adachi, *Optical Constants of Crystalline and Amorphous Semiconductors* (Kluwer, Boston, 1999).
[31]G. Leibiger, B. Rheinlander, J. Sik, and M. Shubert, J. Appl. Phys. **89**, 4927 (2001).
[32]P. Bhattacharya, *Semiconductor Optoelectronic Devices* (Prentice-Hall, Englewood Cliffs, NJ, 1997).
[33]R. Trotta, A. Polimeni, M. Capizzi, F. Martelli, S. Rubini, M. Francardi, A. Gerardino, and L. Mariucci, Appl. Phys. Lett. **94**, 261905 (2009).
[34]G. Bisognin, D. De Salvador, E. Napolitani, M. Berti, A. Polimeni, M. Capizzi, S. Rubini, F. Martelli, and A. Franciosi, J. Appl. Cryst. **41**, 366 (2008).